Cryst. Res. Technol. **39**, No. 1, 11 – 22 (2004) / **DOI** 10.1002/crat.200310143

High temperature arsenic doping of CdHgTe epitaxial layers

A. Vlasov[1], V. Bogoboyashchyy[2], O. Bonchyk*[3], A. Barcz[4]

[1] Ivan Franko National University, Physical Department,49 General Chuprynka Str., 79044, Lviv, Ukraine
[2] Kremenchuk State Polytechnical University, 20 Pershotravneva St., 39614 Kremenchuk, Ukraine
[3] Institute for Applied Problems of Mechanics and Mathematics of NASU,3-b Naukova Str., 79601, Lviv, Ukraine
[4] Institute of Physics of Polish Academy of Sciences, 32/46 Al. Lotnikow, 02-668 Warsaw, Poland

Received 24 March 2003, accepted 10 April 2003
Published online 15 January 2004

Key words doping, diffusion, graded-band-gap structures, CdHgTe.
PACS 85.40.Ry

Experimental results on solid-state arsenic doping of the n-type bulk and ISOVPE epitaxial $Cd_XHg_{1-X}Te$ (X = 0.19÷0.3) alloys are presented. The arsenic doped thin epitaxial $Cd_xHg_{1-x}Te$ films ($n_{As} \approx 5\cdot10^{16}\div1\cdot10^{20}$ cm^{-3}; d =2÷5 µm) obtained by RF sputtering in a mercury glow discharge were used as As diffusion sources. The arsenic diffusion and activation were carried out at temperatures T = 500÷600°C under Hg vapour pressure. Immediately after the high temperature treatment all samples were annealed to annihilate point defects. The SIMS analysis was used for determination of the quantitative admixture distribution of As in the diffusion area. The arsenic electrical activity has been evaluated by means of differential Hall, resistivity and thermo-emf measurements. The analysis of experimental data obtained as well as their comparison with previously obtained results has been performed.

© 2004 WILEY-VCH Verlag GmbH & Co. KGaA, Weinheim

1 Introduction

$Cd_XHg_{1-X}Te$ semiconductor solid solutions are materials, which are widely used for fabrication of highly efficient photodetectors, particularly photodiodes based on p^+-n junctions that can be efficiently used in several standard IR spectral ranges. One of the main technological tasks in this field is formation of stable p^+-n junctions. For this purpose the arsenic diffusion doping is applied which makes it possible to produce large amount of acceptor centers in the epitaxial material grown by the methods of LPE [1], MBE [2] and MOCVD [3]. For the diffusion of As at the required depth and for the activation process to take place, it is necessary to perform the annealing at sufficiently high temperatures (T ≥ 400°C), since As behaves in the $Cd_XHg_{1-X}Te$ crystals as an amphoteric impurity with low mobility. This requires the comprehensive study of electrical properties and mechanisms of As diffusion in $Cd_XHg_{1-X}Te$ with the aim of ensuring the efficient control over the doping process during the device structure fabrication.

By now, several models have been put forward for explanation of the regularities of the As diffusion in $Cd_XHg_{1-X}Te$, but their confirmation needs additional experimental research at the temperatures T ≥450°C [4]. For clearing up the local mechanisms of the As diffusion in $Cd_XHg_{1-X}Te$ crystals, dependencies of the diffusion parameters on temperature, partial pressures of the components, concentration, etc. are commonly studied. The first two of them are the most investigated dependencies in the case of the As diffusion in $Cd_XHg_{1-X}Te$ crystals [5, 6]. Because of this the aim of the paper is the determination of the concentration dependence of As diffusivity by means of studying the As diffusive distribution in $Cd_XHg_{1-X}Te$ single crystals and epitaxial structures in the temperature range T = 500 ÷ 600°C.

* Corresponding author: e-mail: bonchyk@rambler.ru

© 2004 WILEY-VCH Verlag GmbH & Co. KGaA, Weinheim

2 Experimental technique

We have examined the As diffusion in the single crystals and epitaxial layers of narrow-gap $Cd_XHg_{1-X}Te$. The single crystals of $X = 0.19$ and 0.3 were grown by the vertical directional crystallization technique. $Cd_XHg_{1-X}Te$ epitaxial layers ($X = 0.22$-0.26) were obtained by the modified ISOVPE method, namely, the evaporation-condensation-diffusion (ECD) method [7] on the substrates of CdTe single crystals with (111) orientation grown by the Bridgmann technique.

Before the As diffusion the samples were annealed for a long time at Hg-saturated conditions at comparatively low temperatures ($T \leq 300$°C), whereupon they had the n-type of conductivity at 77 K due to uncontrollable impurities. Solid source of As was formed on the surface of investigated samples by the method of epitaxial deposition of a thin $Cd_XHg_{1-X}Te$: As film in RF mercury plasma with discharge localization in a quasiclosed volume [8]. The temperature of the deposition was 235°C. As a sputtering material we used the alloyed targets of CdTe-Te, providing formation of the resulting $Cd_xHg_{1-x}Te$ layer of required composition x.

The As impurity was incorporated into the target during its fabrication. For deposition of the layers with small As concentration (less than 0.01 at. %) we used the target with the As concentration of about $4 \cdot 10^{17}$ cm^{-3}; the layers with high As concentration were deposited from the target doped with As up to 10^{20} cm^{-3}. The impurity content in the epitaxial film was additionally regulated by the size of the target's area. The target was sputtered on the substrate surfaces recently etched in brom-methanol etchant. As a result of the described above procedures the heterostructures shown in Fig.1 have been obtained. Samples S.1, S1.2 were obtained by means of sputtering of the target with maximum impurity concentration $n_{As} \approx 10^{20} cm^{-3}$, and samples S.3, S4, S.5 – with $n_{As} \approx 4 \cdot 10^{17}$ cm^{-3} correspondingly.

The heterostructures prepared this way along with the HgTe single crystal source located at some distance from the heterostructures were rigidly mounted in the hot zone of the quartz ampoule. For ensuring the required Hg vapour pressure regulated by the temperature of the cold zone some amount of liquid Hg was added into the ampoule. The ampoules were evacuated with the help of oil-free pumps down to the residual pressure ~10^{-4} Pa. Then they were loaded into the two-zone resistance furnaces, where the diffusion of the impurity and its activation at T = (500÷600) °C took place during 1 hour. Upon completing the diffusion the temperature of the furnace was reduced to 300°C without ampoule overloading and the samples were annealed further at Hg-saturated conditions during 72 hours for reducing the Hg vacancy concentration formed at the high temperature to the value less than the concentration of uncontrolled impurities. Then the initial state of the undoped base of the layer was restored with respect to the defect structure.

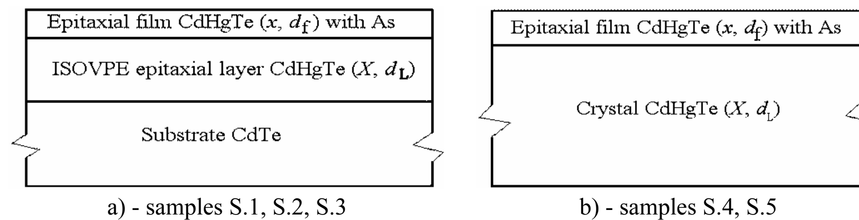

Fig. 1 $Cd_XHg_{1-X}Te$ heterostructures used for investigation of high temperature diffusion of impurity.

Cooling of the ampoules after the treatment was carried out in the resistance furnace immediately after switching it off.

Determination of the conductivity type, carrier concentration ($n = N_d$-N_a) and mobility (μ_n) at 77 K was carried out by the standard Hall measurement technique in the magnetic field range 0÷1.8 T. The composition X of the ECD epitaxial layers and the $Cd_XHg_{1-X}Te$ singles crystals was measured using optical absorption spectra and long wavelength photoconductivity cut-off. The composition x of the As doped $Cd_xHg_{1-x}Te$ films was determined on the test structures obtained on the CdTe substrates by RF sputtering according to the corresponding modes. The total thickness of epitaxial layers that is the sum of thickness of the base undoped layer (d_L) and As doped epitaxial film one (d_f) was measured on the cross cleavage by metallographic

© 2004 WILEY-VCH Verlag GmbH & Co. KGaA, Weinheim

microscope before and after the diffusion process. The electrophysical properties of the samples measured before the source growth, as well as the characteristics of the sources are presented in Table 1.

Quantitative study of the As concentration distribution along the depth of the obtained epitaxial structures was performed on the Cameca IMS−6F device using the standard SIMS technique. This technique was also applied for the observation of the qualitative changes of the composition of $Cd_XHg_{1-X}Te$ solid solution during the interdiffusion of the main components of the doped epitaxial film with the base material; the observation was carried out upon the line of 202Hg133Cs signal obtained using Cs^{133} ions as an primary beam.

The $Cd_XHg_{1-X}Te$ epitaxial layers grown by the ECD technology are characterized by the noticeable band-gap grading. Therefore, the influence of the composition gradient on the As diffusion have been examined here by comparison of diffusion structures obtained in such two cases: when the As concentration gradient was directed towards gap widening, and when it was directed towards gap narrowing. With this aim a thin $Cd_XHg_{1-X}Te$ film with the As concentration of about $4{\cdot}10^{17}$ cm^{-3} (i.e., the As source was the same as for sample S.3) was deposited on the surface of the two structurally perfect $Cd_XHg_{1-X}Te$ single crystal plates with (111) orientation and with compositions X = 0.3 and X = 0.19 (samples S.4 and S.5, respectively). The As up-diffusion was executed in the same conditions as for sample S.3: T = 550°C; P_{Hg} = $3.3{\cdot}10^5$ Pa; t = 1 h. In structure S.4 the composition x of the As source was slightly smaller (x = 0.26), and in the structure S.5 it was larger (x = 0.22). Therefore, due to the interdiffusion of the main components the composition gradient occurred near the surface, with its direction being opposite in these two structures.

Table 1 Summary of electrophysical measurements data.

№	X	d_L, μm	N_d-N_a, cm^{-3}	μ_n, cm^2 V^{-1} s^{-1}	**Diffusant source**		
					x	d_f, μm	n_{As}, cm^{-3}
S.1	0.24	60	$2.8{\cdot}10^{16}$	$2.6{\cdot}10^4$	0.22	7.4	$\approx 10^{20}$
S.2	0.25	58	$2.5{\cdot}10^{16}$	$2.7{\cdot}10^4$	0.22	4.7	$\approx 10^{20}$
S.3	0.22	59	$1.1{\cdot}10^{16}$	$3.2{\cdot}10^4$	0.22	4	$\approx 4{\cdot}10^{17}$
S.4	0.3	800	$3.8{\cdot}10^{14}$	$7.2{\cdot}10^4$	0.26	4	$\approx 4{\cdot}10^{17}$
S.5	0.19	800	$2.3{\cdot}10^{14}$	$2.6{\cdot}10^5$	0.22	3	$\approx 4{\cdot}10^{17}$

For determining the impurity's electrical activity there has been additionally measured the depth (d_j) of the p-n junction location by its direct observation in electron microscope in EBIC regime and by the measurement of thermo e.m.f at T=77K on the test mesa-structures.

3 Experimental results

The profiles of the distribution of As concentration and 202Hg133Cs signal along the depth, which were obtained with the help of the SIMS technique, are shown in Fig.2-5.

The results of measurements for the diffusion structure S.1 formed during the high-temperature diffusion process at T = 600°C and mercury vapour pressure P_{Hg} = $2.3{\cdot}10^5$ Pa are presented in Fig.2. In this figure, the location of the initial metallurgical boundary between the As source and the ECD epitaxial layer is marked. Besides, it is also indicated the background carrier concentration measured by the Hall method in the test sample of structure S.1 obtained after the chemical etching of the layer, the thickness of which exceeds the maximum depth of impurity penetration. The measured value correlates well with the initial carrier concentration in the starting ECD epitaxial layer.

The As distribution profile has a complex nature. Firstly, the As diffusion has occurred not only inwards the sample, but also outwards it; in the surface layer with thickness of about 2μm the As concentration decreased by nearly two orders of magnitude in comparison with the initial concentration in the source. Obviously, the As out-diffusion happens there due to the fact that As is a volatile element, and its partial pressure in the vapour phase is small at the beginning of the process. That is why As sublimates from the solid solution into the

© 2004 WILEY-VCH Verlag GmbH & Co. KGaA, Weinheim

vapour phase and the surface concentration of the mobile As form decreases to the value which corresponds to the equilibrium condition.

Secondly, in the As distribution profiles both on the left and on the right side of the metallurgical boundary there are clearly seen several regions with different rates of the diffusion processes which are denoted here as (A), (B) and (G). It is clear that at low concentrations of As (< 10^{18} cm^{-3}, region B) the diffusion coefficient is much larger than at high concentrations (regions A and G).

Thirdly, the As distribution profile is strongly asymmetric. In its right part near the metallurgical boundary there is a distinct region (G) with the intermediate value of diffusion coefficient, which is totally absent in the region of out-diffusion. This points at the structural inhomogeneity of the As source and leads to the assumption that either a getter is connected with the metallurgical boundary which accumulates and binds the As impurity, or there are an additional source in which As is in the other (bound) form and diffuses irrespectively of the rest of the impurities. Fitting by the Gauss curve shows that in the region of the peak there are ~$5\cdot10^{15}$ cm^{-2} As atoms. In the left part of the profile we additionally observe the surface gettering of As; in the surface layer of the structure with the thickness ~0.1 μm the As concentration sharply increases.

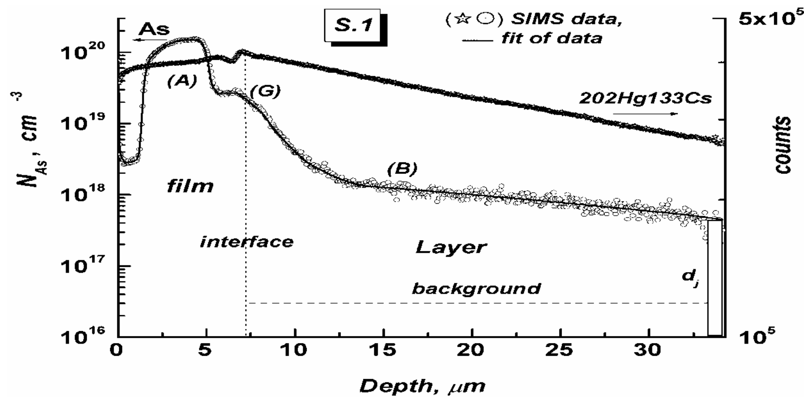

Fig. 2 SIMS distribution of As and Hg concentrations in surface regions for heteroepitaxial structure of sample S.1: T = 600°C; P_{Hg} = $2.3\cdot10^5$ Pa; the treatment in the diffusion regime for one hour.

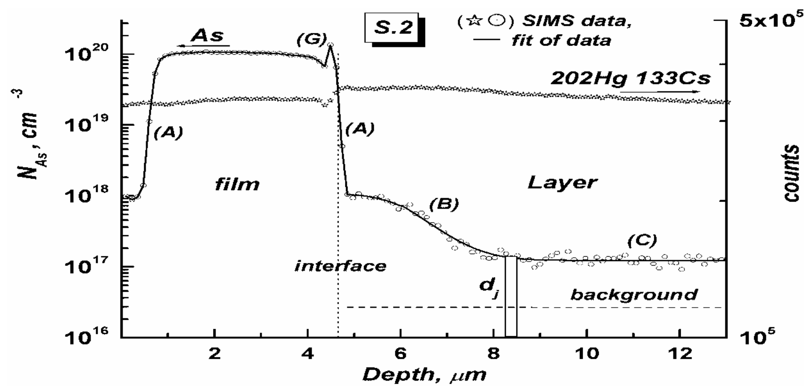

Fig. 3 SIMS distribution of As and Hg concentrations in surface regions for heteroepitaxial structure of sample S.2: T= 500°C; P_{Hg} = $2.9\cdot10^5$ Pa; the treatment in the diffusion regime for one hour.

The *p-n* junction in structure S.1 lies in the region of the profile where the impurity concentration greatly exceeds the free carrier concentration of the n-base at 77 K (see Fig.2). This is evidence of low average electrical activity of As near the p-n junction and in the depth of the epitaxial structure (~10% and even lower). Thus, the significant part of As atoms in the inner region of the structure is either in the form of neutral complexes [9], or decorates the extended defects [10].

Fig.3 illustrates the SIMS profiles for structure S.2 obtained at T = 500°C and P_{Hg} = $2.9\cdot10^5$ Pa. It is seen that as in the previous experiment the level of 202Hg133Cs signal decreases towards the surface, but due to the temperature decrease and some pressure increase the composition gradient in the diffusion region of structure

© 2004 WILEY-VCH Verlag GmbH & Co. KGaA, Weinheim

S.2 turns out to be smaller. The As distribution profile in this case consists, as earlier, of the two parts: in the left part As diffuses outside (out-diffusion), and in the right part As diffuses inwards the sample. In each part one can distinguish two regions, which correspond to the fast (A) and slow (B) impurity diffusion components. Moreover, in the right part of the profile there appears the additional third component (C) that corresponds to the superfast diffusion of As. In this region downturn of As concentration due to up-diffusion is practically unmeasurable, however, the concentration values here are two orders of magnitude larger than the concentration of uncontrollable As; this indicates that region C also is the region of diffusion profile. To the contrary of the previous case, the peak of As concentration at the metallurgical boundary of structure S.2 stands out quite distinctively and exceeds its level in the rest of the source, which points to the existence of

the additional source of the bound As near this boundary. The peak is significantly narrower than in sample S.1 which indicates the large activation energy of bound As; the amount of accumulated As is 3 times less than in the previous case.

As in sample S.1, p-n junction in structure S.2 is located at the boundary of the regions of fast (B) and superfast (C) diffusion, with the As concentration in C region being several times larger than the residual electron concentration which practically coincides with its initial value (before doping) and therefore is determined by uncontrolled impurities. This is an evidence of high electrical activity of As in the region of fast diffusion B and of slow activity in region C.

The presence of several regions of the profile of diffusion distribution of the impurity with different diffusion coefficients indicates, as a rule, either the presence of several independent diffusion mechanisms, or the dependence of diffusion coefficient on the impurity concentration. These two cases can be distinguished when investigating the impact of impurity concentration in the source on the diffusion distribution of the impurity.

Fig.4 presents the results of experimental research carried out for the diffusion structure S.3 which was formed at the intermediate temperature $T = 550°C$ and the Hg partial pressure $P_{Hg} = 3.3{\cdot}10^5$ Pa using the source where the impurity concentration was smaller by two orders of magnitude ($\approx 4{\cdot}10^{17}$ cm^{-3}). It is clear that increasing the Hg vapour pressure during the up-diffusion up to $3.3{\cdot}10^5$ Pa causes a change of the nature of the distribution of composition X neighboring to the surface; there is some increase in the level of 202Hg133Cs signal when approaching the sample surface. In this sample the most part of the source has dissolved due to the processes of out-diffusion and sublimation of As, and also due to the impurity diffusion inwards the structure. However, the dilution of the source did not take place completely.

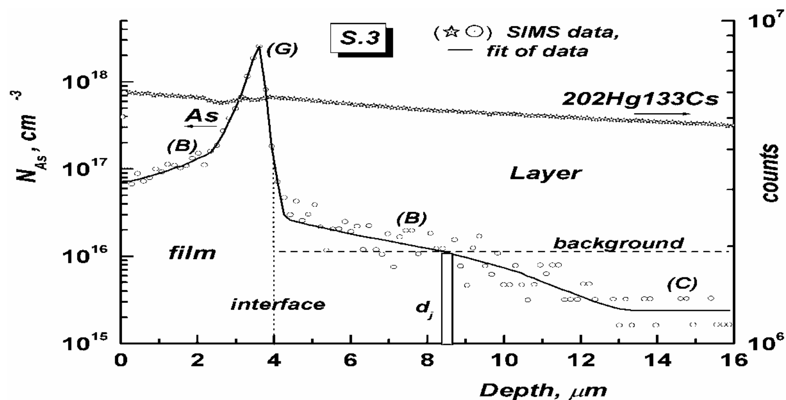

Fig. 4 SIMS distribution of As and Hg concentrations in surface regions for heteroepitaxial structure of sample S.3: $T = 550°C$; $P_{Hg} = 3.3{\cdot}10^5$ Pa; the treatment in the diffusion regime for one hour.

The asymmetric structure of the concentration peak formed near the metallurgical boundary attests that the peak is actually doubled. The main peak located at the depth ~3.5 μm is 5 times higher than the level of initial concentration of As in the source, and the total amount of As in the peak region exceeds the As initial amount in the source and equals to $1.5{\cdot}10^{14}$ cm^{-2}. That is why this peak is unambiguously associated with the As additional source. The second peak's top slighly stands out against a background of the main peak at the depth from 3 to 3.5 μm, and this peak is a residue of the source with As concentration of about $4{\cdot}10^{17}$ cm^{-3}.

© 2004 WILEY-VCH Verlag GmbH & Co. KGaA, Weinheim

Estimations show that the part of the source located at the depth 3.5-4 μm is dissolved in the sample, because the amount of As in the part of the source of thickness 0.5 μm and obtained from the diffusion profile As amount that is diluted in the initial film both are equal to $2\cdot10^{13}$ at/cm^2.

In contrast to the two previous cases, the p-n junction in structure S.3 is located within the region of fast diffusion B, with As concentration in the p-n junction region being practically equal to the concentration of impurity electrons which is determined by the uncontrolled impurities. This means that in the region of fast diffusion As shows the high electric activity of predominantly acceptor type which is close to 100%.

Fig.5 demonstrates the results of investigation of influence of the composition gradient on the As diffusion in $Cd_XHg_{1-X}Te$. The procedure of fabrication of samples S.4 and S.5 has been described in detail above. The investigation shows that the composition gradient in those two structures was opposite that are indicated by the SIMS profiles of samples S.4 and S.5 obtained from the lines of 202Hg133Cs signal (Fig.5a.b). Since the Hg interdiffusion coefficient in $Cd_XHg_{1-X}Te$ (X = 0.2-0.3) is several orders of magnitude greater than the As diffusivity [11], the As diffusion occurs practically at a constant composition gradient. Though the distribution of electrically active impurity should be subjected to the influence of built-in fields [12], one can see, that in these experiments we do not observe such effect: for both structures the As diffusivity turns out to be approximately the same. Such result can be obviously explained by the small values of band-gap gradients in the initial heterostructures. The results of fitting performed by the means of least square approximation indicate that As diffusivity in structures S.4 and S.5 at temperature 550°C does not depend on As concentration and equals to $D_{As} \approx 5{,}5\cdot10^{-11}$ cm^{2}s^{-1}. Having determined D_{As} we have taken into account that in the current case the source was entirely diluted during the up-diffusion, therefore there occurred the diffusion from a finite source of limited width [13], so the experimental profile of As distribution in structures S.4 and S.5 almost in the whole investigated depth of the layer had the Gauss shape. At the same time, at the depth larger than 15-17 μm there is observed a tail related to the superfast diffusion component. Like in the sample S.3, the As concentration in this region is $(2\div3)\cdot10^{15}$cm^{-3} which is several times larger than the uncontrolled As concentration in the $Cd_XHg_{1-X}Te$ single crystals under study. Like in the previous cases the accumulation of As takes place near the surface and metallurgical boundary. However, the total amount of As which is bound near the metallurgical boundary is small enough and equals to ~10^{13}cm^{-2}.

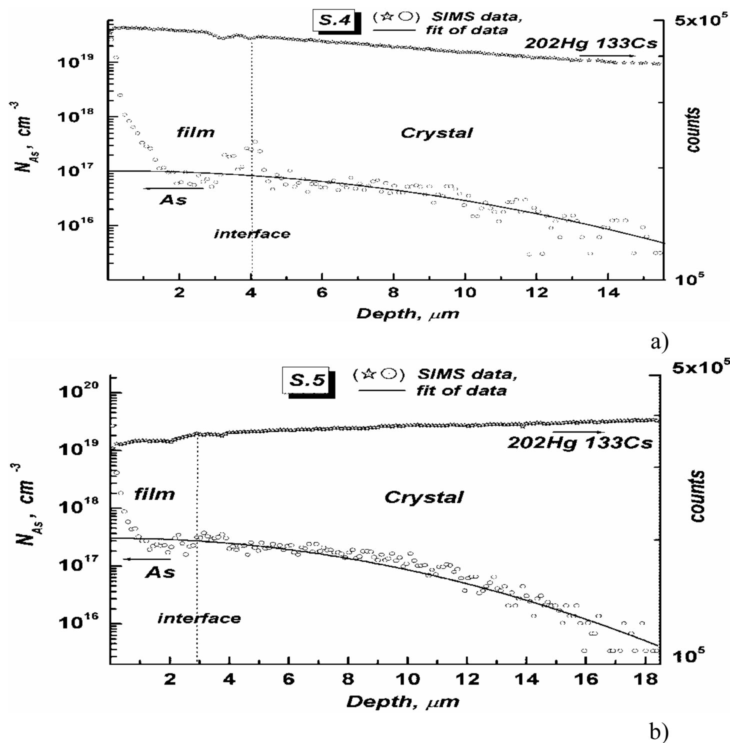

Fig. 5 SIMS distribution of As and Hg concentrations in surface regions for a) – S.4; b) –S.5: T = 550°C; P_{Hg} = $3{,}3\cdot10^5$ Pa; the treatment in the diffusion regime for one hour.

© 2004 WILEY-VCH Verlag GmbH & Co. KGaA, Weinheim

4 Discussion

The distribution profiles of As have a complicated nature which are the evidence of simultaneous presence of several mechanisms of As penetration in $Cd_XHg_{1-X}Te$. There is a concentration peak at the metallurgical boundary of the structure and the three regions (A, B, C) on the diffusion profile which are characterized by the substantially different values of the diffusion coefficient. At a small level of doping (region B) the profile of As distribution has a classical form resulted from the Fick laws which conforms well with the experimental data [5]. Below, we propose an explanation of the mentioned above peculiarities of the diffusion structures.

(i) The concentration peak of As at the metallurgical boundary is observed in all cases and, obviously, is a consequence of inhomogeneity of the As source obtained by the applied method. The peak halfwidth rapidly increases when the temperature of the diffusion process rising, and height of the peak clearly correlates with the As concentration in the source. The total amount of As accumulated in this peak ranges from about 10^{13} cm^{-2} (structures S.4-S.5) to $5{\cdot}10^{15}$ cm^{-2} (sample S.1), and in some cases (sample S.3) exceeds the amount of As in the rest part of the source. As this peak occurs even at high As concentration and relatively low temperatures when the As diffusion directly in the source is very weak and it can not cause significant As segregation, these experimental data can be consistently explained by formation of such peak during depositing the source due to the presence on the surface of the layer enriched with As. This assumption is also substantiated by the existence of an enriched surface layer in the structures shown in Fig. 2-5. Arsenic in the additional source is in another (bound) form and diffuses independently of other impurities. This requires careful analysis of the diffusion profile of As. It is clear that such analysis can be correctly made only beyond the region of the bound impurity, i.e. in regions A, B, C.

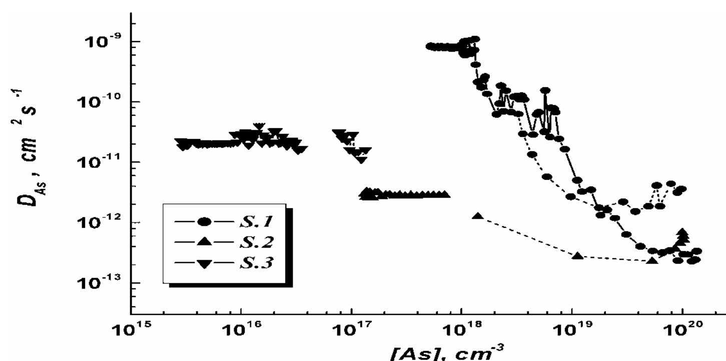

Fig. 6 Arsenic diffusion coefficient at different temperatures versus arsenic concentration: points – experimental data; curves – results of calculation: ······ internal part of the profile, —— external part of the profile.

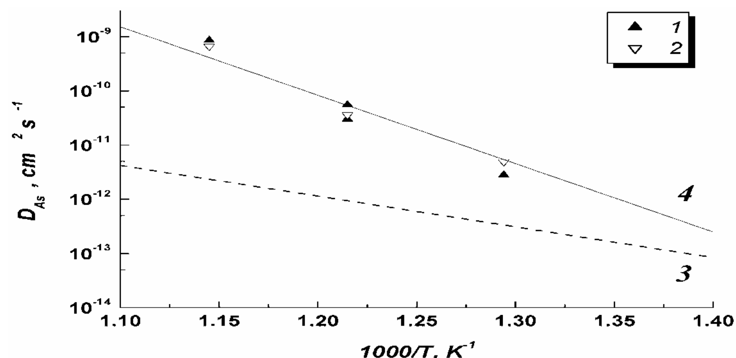

Fig. 7 Arsenic diffusion coefficient versus temperature at low arsenic concentrations: points {1} – experimental data; points {2 } – results of calculation by formula (2) for conditions of the experiment, lines: results of calculation by formula (2) for saturated Hg vapour – {3} and average pressure P_{Hg} = $2.8{\cdot}10^5$ Pa – {*4*}.

(ii) Comparison of the profiles shown in Fig.2-5 shows that in regions A and B of the diffusion profile the diffusion coefficient is different in different ranges of As concentration. This phenomenon is possible in two cases: either As diffusion coefficient depends on the concentration, or there takes place a multi-component diffusion. In the first case one can use the Boltzmann-Matano method for determining D_{As} vs. As

© 2004 WILEY-VCH Verlag GmbH & Co. KGaA, Weinheim

concentration. The results of such analysis are shown in Fig.6. It is clear that at As concentration [As] < 10^{18} cm^{-3} D_{As} is practically independent of [As]. On the other hand, at first it rapidly decreases with [As] rising above 10^{18} cm^{-3} (in particular, as $1/[As]^2$ at T = 600°C), but then (at [As] > 10^{19} cm^{-3}) the value of D_{As} is stabilized again. One can see that the D_{As} temperature dependence at low concentrations of As (region B) being much stronger than that at high [As] (region A). Analysis of the temperature dependence of D_{As}, performed in region B of the profile at [As] < 10^{18} cm^{-3} by using the least square method, gives the following expression:

$$D_{As}^{(B)} = 7.7\cdot 10^{-9} exp(-3.3\ eV/kT)\ cm^2s^{-1}. \quad (1)$$

The comparison of the results with those presented in [5-6] (see Fig.7) shows that the diffusion coefficient $D_{As}^{(B)}$ exactly corresponds to the value of D_{As} found in [5-6]. Indeed, according to [6] at the Hg-saturated conditions at the temperature below 450°C:

$$D_{As} = (7.76 \overset{\times}{\underset{\div}{}} 1.1)\cdot 10^{-6} exp(-1.13\pm 0.01\ eV/kT)\ cm^2s^{-1}; \quad (2)$$

(line *3* in Fig. 7). Taking into account that at high partial pressures of Hg $D_{As} \propto [V_{Hg}'']/P_{Hg}^2$ [6], where $[V_{Hg}'']$ is the concentration of the double charged Hg vacancies, one can make sure that the result of interpolation of the data [5-6] in the region of high temperature for the medium pressure $P_{Hg} = 2.8\cdot 10^5$ Pa is close to values $D_{As}^{(B)}$ (line *4* in Fig. 7) obtained there. The V_{Hg}'' concentration in the conditions of the experiment described here and in the conditions of a saturation with Hg was calculated on the basis of experimental data of the authors [14]; it has been taken into account that in the region of fast diffusion $[As] << n_i$, where n_i is the intrinsic electron concentration.

Thus, the mechanism of the fast diffusion at T > 500°C is the same as at $T \leq$ 425°C [5]. This allows using directly the experimental data of [5] for determining the main features of the As fast diffusion:

a) according to [5], at high pressures $D_{As} \propto 1/P_{Hg}^3$, whereas at low pressures $D_{As} \propto 1/P_{Hg}$;

b) in the diffusion region the acceptor defects are predominant ones at high pressures ($P_{Hg} \approx 3\cdot 10^5$ Pa in our case);

c) at low As concentration D_{As} is independent of [As], whereas at [As] > 10^{18} cm^{-3} D_{As} rapidly decreases at rising [As].

The last fact conforms well to the data of [5] according to which D_{As} is independent of [As] if [As] < $5\cdot 10^{18}$ cm^{-3} at high Hg vapour pressure (namely, $P_{Hg} > 1.1\cdot 10^4$ Pa at 350 – 425°C). It should be mentioned that at lower pressures the profiles of As were not described by the erfc-function. The authors [5] suppose that a multi-component diffusion mechanism of diffusion is realized in their experiment. On the basis of the own experimental data the authors [5] put forward an assumption that the As diffusion occurs through the formation and migration of the mobile defects of the As_{Hg} type. They assume that the substitution centers of the As_{Hg} type are the single charged donors ($As^{\cdot}_{Hg}$) and the substitution centers of the As_{Hg} type are the single charged acceptors (As'_{Te}). Besides, there has been considered the existence of substantial amount of the double charged Hg vacancies V_{Hg}''.

The detailed analysis of this and other proposed mechanisms has been made by Shaw in [4, 6]. According to this analysis among all known models the only mechanism, which is the movement of the $As^{\cdot}_{Hg}$ cations via vacancy mechanism, can explain the character of D_{As} change with P_{Hg} which is observed in $Hg_{0.8}Cd_{0.2}Te$.

There are several versions of such vacancy mechanism [4]. According to the first version, proposed by Chandra et al. [5], the jumps of $As^{\cdot}_{Hg}$ occur only in the sites of the cation sublattice, and only then when in the first coordinate sphere the V_{Hg}'' is present. After the jump the vacancy can move far from the given site and then $As^{\cdot}_{Hg}$ has to wait when another cation vacancy appears in the first coordinate sphere. According to the second model (Berding et al. [15]), the mercury vacancy and $As^{\cdot}_{Hg}$ can form the neutral complexes $A^{\times} = (As_{Hg}V_{Hg})^{\times}$, which move as a single whole, however, according to [15], the vacancy is a single charged defect. Shaw [4] adds the third possibility - the creation and diffusion of the acceptor complex $A' = (As_{Hg}V_{Hg})'$.

© 2004 WILEY-VCH Verlag GmbH & Co. KGaA, Weinheim

All these mechanisms qualitatively explain the revealed in [5] features of the As diffusion, namely: in these models $D_{As} \propto 1/P_{Hg}^3$ at high Hg vapour pressure and $D_{As} \propto 1/P_{Hg}$ at low P_{Hg}, and D_{As} is independent of the As concentration at low doping. But the conclusions contradict to the found concentration dependence of D_{As} at high doping. Thus, according to [4], in the first model at the extrinsic conditions the As diffusivity should either increase simultaneously with the concentration rising if [As] = $[As^{\cdot}_{Hg}] > n_i >> [As'_{Te}]$, or be independent of the concentration if [As] = $[As'_{Te}] > n_i >> [As^{\cdot}_{Hg}]$. The same result we obtain when $[As'_{Te}] = [As^{\cdot}_{Hg}] = 0.5$ [As]; in this case the concentrations of both holes and V_{Hg}'' do not depend on [As], and that's why D_{As} does not depend on [As]. Actually it follows from the experimental data that $D_{As} \propto 1/[As]^2$ at $[As] > n_i$ (see Fig. 6). On the other hand, the model [6] contradicts to the experimental data concerning the charge state of the main defects in the fast diffusion region. According to [6], at $T > 500°C$ and $P_{Hg} > 1\cdot10^5$ Pa the centers of the $As^{\cdot}_{Hg}$ type have to dominate over As'_{Te}, whereas the experiment shows that in the fast diffusion region, on the contrary, the acceptors are predominant. This conclusion is confirmed by the results obtained in [16], where it has been shown that the doped with As $Cd_{0,2}Hg_{0,8}Te$ crystals annealed at $P_{Hg} > 1\cdot10^5$ Pa have acceptor type of conductivity irrespectively of the temperature. The same situation takes place when As diffusion occurs by means of the creation and migration both of the $A^{\times}$ and A' complexes: accordingly to these models the diffusivity has to increase with concentration rising at $[As] > n_i$.

For identification of the mechanism of the fast diffusion of As in $Cd_XHg_{1-X}Te$, which corresponds to region B of the diffusion profile, we have carried out numerical calculation of D_{As}. The calculation has been performed in the limits of the model in which the main defects are As'_{Te}, Hg vacancy, V_{Hg}'' as well as $As_{Hg}^{\nu\cdot}$ and complex $A^{\mu'} = (As_{Hg}V_{Hg})^{\mu'}$. The charge states of the last defects ν and μ, respectively, were considered as a fitting parameter. The corresponding quasi-chemical reactions and mass action laws are presented in Table 2. Here, N_V is the integral density of the states in valence band; K_{As}, K_V are the respective constants of equilibrium state. When writing the fourth equation we assumed that the vacancy ionization energy is near to zero due to the strong screening.

Table 2 The main quasichemical reaction of defect formation and electroneutrality conditions in $Cd_XHg_{1-X}Te$.

	Reaction	Law of mass action
1	$As_{Hg}\nu^{\cdot} = As'_{Te} + 2V_{Hg}\times + (\nu+1)h^{\cdot}$	$[As_{Hg}\,\nu^{\cdot}] = K_{As}\,[As'_{Te}]\,(p/n_i)\,\nu^{+1}\,[V_{Hg}\times]^2$
2	$A^{\mu\,\prime} + (\mu\text{-}1)h^{\cdot} = As'_{Te} + 3V_{Hg}\times$	$(p/n_i)^{\mu\,\text{-}1}\,[A^{\mu\prime}] = K_A\,[As'_{Te}]\,[V_{Hg}\times]^3$
3	$Hg(V) + V_{Hg}\times = 0$	$[V_{Hg}\times = K_V/P_{Hg}$
4	$V_{Hg}\times = V_{Hg}'' + 2h^{\cdot}$	$[V_{Hg}''] = (K_V/\,6P_{Hg})\times(N_V/p)^2$
5	$e' + h^{\cdot} \to 0$	$pn = n_i^2$
6	Electroneutrality condition	$p - n = [As'_{Te}] + \mu[A^{\mu\,\prime}] - \nu\,[As_{Hg}\nu^{\cdot}] + 2[V_{Hg}'']$

From this model of the defect structure we obtain:

$$\alpha_1(p) = [As_{Hg}^{\nu\,\cdot}]/[As] = (p/n_i)^{\nu+1}(P_1/P_{Hg})^2/[1+(p/n_i)^{\nu+1}(P_1/P_{Hg})^2 + (p/n_i)^{1-\mu}(P_2/P_{Hg})^3]; \quad (3)$$

$$\alpha_2(p) = [A^{\mu\,\prime}]/[As] = (p/n_i)^{1-\mu}(P_2/P_{Hg})^3/[1+(p/n_i)^{\nu+1}(P_1/P_{Hg})^2 + (p/n_i)^{1-\mu}(P_2/P_{Hg})^3]; \quad (4)$$

$$\beta(p) = [As] = [p - n_i^2/p - 2(K_V/\,6P_{Hg})\times(N_V/p)^2] \times [1+(p/n_i)^{\nu+1}(P_1/P_{Hg})^2 + (p/n_i)^{1-\mu}(P_2/P_{Hg})^3] \times$$
$$\times [1-\nu\,(p/n_i)^{\nu+1}(P_1/P_{Hg})^2 + \mu(p/n_i)^{1-\mu}(P_2/P_{Hg})^3]^{-1}; \quad (5)$$

where the notations $P_1 = K_V\,(K_{As})^{S}$; $P_2 = K_V\,(K_A)^{1/3}$ are introduced.

The As diffusivity for the first and second versions of the vacancy mechanisms was written in accordance with [4]:

$$D_{As}^{(1)} = D(As_{Hg})\{\,\partial[As_{Hg}^{\nu\,\cdot}]/\,\partial x + \nu G[As_{Hg}^{\nu\,\cdot}]\}/\,\partial\,[As]/\,\partial x\,; \quad (6)$$

© 2004 WILEY-VCH Verlag GmbH & Co. KGaA, Weinheim

$$D_{As}^{(2)} = D(\mathrm{A})\{ \partial[\mathrm{A}^{\mu}{}']/ \partial x - \mu G[\mathrm{A}^{\mu}{}']\}/ \partial [\mathrm{As}]/ \partial x \; ; \tag{7}$$

where $G = eE/kT$ (e is the electron charge; E is the electric field strength; k is the Boltzmann constant).

After the substitution of Eqs. (3)-(5) into formulas (6)-(7) and considering that $G = (1/p)\, \partial p/\partial x$ one can obtain:

$$D_{As}^{(1)} = D(\mathrm{As_{Hg}})\{ \alpha_1 + \alpha_1 (\beta /p)/(\partial \beta/ \partial p) + \beta (\partial\alpha_1/\partial p)/(\partial \beta/ \partial p)\} \; ; \tag{8}$$

$$D_{As}^{(2)} = D(\mathrm{A})\{ \alpha_2 + \alpha_2 (\beta/p)/(\partial \beta/ \partial p) + \beta(\partial\alpha_2/\partial p)/(\partial \beta/ \partial p)\} \; . \tag{9}$$

It is clear that at low impurity concentration independently of the charge state of defects in both models at high pressure $D_{\mathrm{As}} \propto 1/P_{\mathrm{Hg}}^3$ and at low pressure $D_{\mathrm{As}} \propto 1/P_{\mathrm{Hg}}$. When calculating $D_{As}^{(1)}$ i $D_{As}^{(2)}$ the expressions for $D(\mathrm{As_{Hg}})$ i $D(\mathrm{A})$ are written in the form presented in [4]:

$$D(\mathrm{A}) = 2d^2 w_1 w_2/(w_1 + w_2) = D_V\, w_1 w_2/[(w_1 + w_2)w_0]; \tag{10}$$

$$D\,(\mathrm{As_{Hg}}) = 2d^2(f w_2 w_4/w_3)\, [\mathrm{V_{Hg}}'']\, /\, S = D_V\, [f w_2 w_4/(w_0\, w_3)]\, [\mathrm{V_{Hg}}'']\, /\, S. \tag{11}$$

Here, d is the lattice parameter; f is the correlation factor; w_0 is the exchange rate of a vacancy with an intrinsic cation in the pure lattice; w_1 is the exchange rate of a vacancy located in the first coordination sphere at a nearest-neighbour site to $\mathrm{As_{Hg}}$ with an intrinsic cation located in the first coordination sphere for both the vacancy and $\mathrm{As_{Hg}}$; w_2 in the exchange rate of $\mathrm{As_{Hg}}$ and vacancy in the first coordination sphere; w_3 is the exchange rate of a vacancy with an intrinsic cation from the second and third coordination spheres relative to $\mathrm{As_{Hg}}$; w_4 is the exchange rate of a vacancy with an intrinsic cation in the first coordination sphere for $\mathrm{As_{Hg}}$; D_V in the diffusion coefficient of the vacancies; $S = 1.48 \cdot 10^{22}$ cm^{-3} is the concentration of cationic sites. The results of calculations of D_{As} are shown in Fig. 8. It has been assumed during the calculations that:

$$D_V = 0.0063 \exp\left(-0.85\, eV/k_B T\right)\ \mathrm{cm^2 s^{-1}}\ ;\ K_V P_{Hg}^{\circ} = 2.16 \cdot 10^{23} \exp(-1.49\ \mathrm{eV/kT})\ \mathrm{cm^{-3}}\ . \tag{12}$$

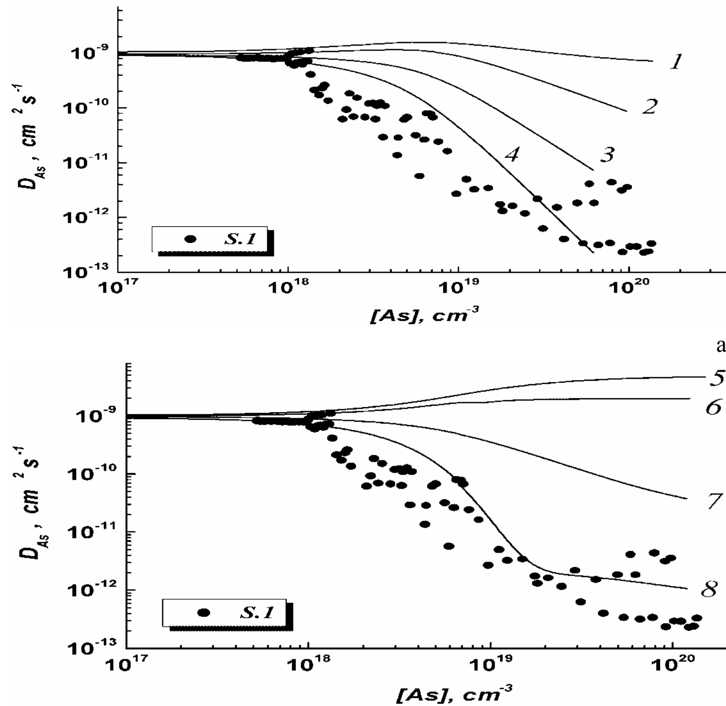

Fig. 8 Arsenic diffusion coefficient at 600°C versus arsenic concentration:
a): *1* - $\nu = 1$; $P_1/P_{\mathrm{Hg}} = 0.1$; $P_2/P_{\mathrm{Hg}} = 0$; $f w_2 w_4/(w_0 w_3) = 1000$;
2 - $\nu = 0$; $P_1/P_{\mathrm{Hg}} = 0.1$; $P_2/P_{\mathrm{Hg}} = 0$; $f w_2 w_4/(w_0 w_3) = 3000$;
3 - $\nu = -1$; $P_1/P_{\mathrm{Hg}} = 0.1$; $P_2/P_{\mathrm{Hg}} = 0$; $f w_2 w_4/(w_0 w_3) = 10000$;
4 - $\nu = -2$; $P_1/P_{\mathrm{Hg}} = 0.1$; $P_2/P_{\mathrm{Hg}} = 0$; $f w_2 w_4/(w_0 w_3) = 35000$;
b): *5* - $\mu = 0$; $\nu = 1$; $P_1/P_{\mathrm{Hg}} = 0.007$; $P_2/P_{\mathrm{Hg}} = 0.5$; $w_1 w_2/[(w_1 + w_2)w_0] = 0.05$;
6 - $\mu = 1$; $\nu = 1$; $P_1/P_{\mathrm{Hg}} = 0.007$; $P_2/P_{\mathrm{Hg}} = 0.5$; $w_1 w_2/[(w_1 + w_2)w_0] = 0.14$;
7 - $\mu = 2$; $\nu = 1$; $P_1/P_{\mathrm{Hg}} = 0.007$; $P_2/P_{\mathrm{Hg}} = 0.5$; $w_1 w_2/[(w_1 + w_2)w_0] = 0.45$;
8 - $\mu = 3$; $\nu = 1$; $P_1/P_{\mathrm{Hg}} = 0.007$; $P_2/P_{\mathrm{Hg}} = 0.5$; $w_1 w_2/[(w_1 + w_2)w_0] = 1.5$.

© 2004 WILEY-VCH Verlag GmbH & Co. KGaA, Weinheim

(the experimental data of [14]). Here, $P_{Hg}°$ is the Hg saturated vapour pressure. The coefficients $w_1w_2/[(w_1 + w_2)w_0]$, $fw_2w_4/(w_0 w_3)$, P_1, P_2 are considered to be the fitting parameters. Concentration of the intrinsic electrons (n_i = $1.1\cdot10^{18}$ cm^{-3}) was calculated on the basis of the data from [16]. It is clearly seen that the results of calculations conform best to the experiment for the model in which the As transfer occurs via either the triple charge acceptor complex A′′′ (curve 8), or the substitution center As_{Hg}'' (curve 4). However there exists a substantial difference between these models. In the case of the A′′′ complexes the model can be well adjusted with the experiment taking the following value of the frequency factor: $w_1w_2/[(w_1 + w_2)w_0] \sim 1$, i.e. at $w_1 \sim w_0$ and $w_2 \sim w_0$ which is entirely correct from the physical point of view. Besides, in the limits of this model one can easily explain the stabilization of D_{As} during high doping: here, due to the self-compensation the electroneutrality condition has the form $[As'_{Te}] = [As^{\cdot}_{Hg}] = 0.5[As]$, so, p and correspondingly [A′′′] and D_{As} do not depend on [As]. In the case of the As_{Hg}'' substitution center for obtaining the required dependency on the pressure one must take $P_1/P_{Hg} \sim 0.1$ or less, therefore $w_2w_4/(w_0 w_3) > 10^5$. On the other hand, from the Eqs. (10)-(12) it follows that $w_0 \sim 10^{-5}\ \Gamma_0$ at T = 600°C, where Γ_0 is the characteristic frequency of atom oscillation in the crystal lattice, i.e. the value $w_2w_4/(w_0 w_3) \sim 10^5$ corresponds to about-zero activation energy of a jump of As_{Hg}'' into the vacancy that contradicts to the typical values of barrier energy for such processes. Thus, the most probable mechanism of the fast diffusion of As is a migration of the A′′′ = $(As_{Hg}V_{Hg})'''$ complexes. Creation of such a center one can explain in the following way. One atom of Te in the anion sites corresponds to each defect in the cation sublattice – As_{Hg} and $V_{Hg.}$ When the V_{Hg} emerges in the nearest site to As_{Hg}, the uncoupled atom of Te destroys the bond As – Te and forms the double molecular bond Te – Te with the liberated atom of Te. Therefore three uncoupled valence electrons of the As_{Hg} atom provide three acceptor levels of such a center.

(iii) The superfast diffusion is characterized by the following features.

Firstly, this component is peculiar to all the samples. In structures S.1 and S.2 the As concentration in the region of superfast diffusion differs approximately in two times only, thus, in the range 500-600°C it slightly depends on the temperature. On the other hand, in samples S.3-S.5 it is two orders of magnitude smaller than in samples S.1-S.2, where the concentration of As in the source was two orders of magnitude higher. Since samples S.3-S.5 were annealed at the temperature intermediate with respect to S.1-S.2, and the change of pressure was so small that it couldn't influence on the number of defects, it follows that As concentration in the region of superfast diffusion is approximately proportional to the As concentration in the source.

Secondly, in the region of superfast diffusion the concentration of impurity carriers practically coincides with their concentration before the doping, thus, in this region As is passive. On the other hand, in samples S.1-S.2 *p-n* junction lies at the boundary of the regions of fast and superfast diffusion, and in sample S.3 the activity of As is equal to 100%. Hence it follows the conclusion that in the region of fast diffusion As is active. Consequently, these two types of diffusion mechanisms realize different types of defects.

Thirdly, there is no interaction between these types of defects: if they could transform into each other the equilibrium between them would have been established at the expense of such transformations, and the transition point from one region to another would have been the point of changing the diffusion mechanism and the As concentration there would have been determined by the temperature and pressure, rather than by the concentration of As in the source. Taking into account the passive state of As in the region of superfast diffusion, one can suppose that the superfast component corresponds to the enhanced diffusion of As along the extended defects of the structure.

Hence, we may conclude that beyond the limit of the additional peak occurring at the metallurgical boundary the diffusion of As comes about by the several independent ways.

5 Conclusions

1. The investigation of high temperature diffusion of As in $Cd_XHg_{1-X}Te$ from the source obtained by the epitaxial deposition of $Cd_XHg_{1-X}Te$: As in the RF plasma with the discharge localization in a quasi-closed volume indicates the substantial concentration dependence of the As diffusivity at high doping.

© 2004 WILEY-VCH Verlag GmbH & Co. KGaA, Weinheim

2. The diffusion of As in the ECD $Cd_XHg_{1-X}Te$ epitaxial layers at high temperatures is a multi-component process.
3. At the metallurgical boundary between the source and the $Cd_XHg_{1-X}Te$ layers there is As in the bounded state that diffuses independently of other impurities.
4. The fast diffusion component is responsible of a *p-n* junction formation and occurs due to creation and diffusion of the $(As_{Hg}V_{Hg})'''$ acceptor centers. In this region of the diffusion profile As is electrically active is almost 100%.
5. In the region of a superfast diffusion As is in a passive form; most likely, this component of the profile corresponds to the enhanced diffusion of As along the extended defects of the structure.

References

[1] L. O. Bubulac, D. S. Lo, W. E. Tennant, D. D. Edwall, J. C. Chen, J. Ratusnik, J. L. Robinson, and G. Bostrup, Appl. Phys. Let. **50**(22), 1586 (1987).
[2] J. M. Arias, J. G. Pasko, M. Zandian, S. H. Shin, G. M. Williams, L. O. Bubulac, R. E. DeWames, and W. E. Tennant, Appl. Phys. Let. **62**(9), 976 (1993).
[3] L. O. Bubulac, S. J. Irwine, E. R. Gerther, J. Bajaj, W. P Lin, and R. Zucca, Semicond.Sci.Technol. **8**, 270 (1993).
[4] D. Shaw, Semicond.Sci.Technol. **15**, 911 (2000).
[5] D. Chandra, M.W. Goodwin, M.C Chen, and J.A. Dodge, J. Electron. Mater. **22**(8), 1033 (1993).
[6] D. Shaw, Semicond. Sci. Technol. **9**, 1729 (1994).
[7] V. G. Savitsky, O. P. Storchun, Thin Solid Films. **317**, 105 (1998).
[8] V. G. Savitsky, L. G. Mansurov, M. V. Miliyanchuk, B. O. Simkiv, *Copyright USSR* #1480362, 04.08.1987.
[9] T. S. Lee, J. Garland, C. H. Grein, M. Sumstine, A. Jandeska, Y. Selamet, S. Sivananthan, J. Electron. Mater. **29**(6), 869 (2000).
[10] L. O. Bubulac, D. D. Edwall, and C. R. Viswanathan, J. Vac. Sci. Technol. **B9** (3), 1695 (1990).
[11] N. N. Berchenko, V. E. Krevs, V. G Sredin, Semiconductor solid solutions and their applications (in Russian), Moskow, 1982.
[12] L. S. Monastyrsky, B. S. Sokolovsky, Ukr. Fiz. Zur. **39**(2), 242 (1994).
[13] B. I. Boltaks, Diffusion in semiconductors (in Russian), Moskow, 1961.
[14] V. V. Bogoboyashchyy. - to be published.
[15] M. A. Berding, A. Sher, Phys. Lett. **74**(5), 685 (1999).
[16] S. H. Shin, J. M. Arias, M. Zandian, J. G. Pasko, L. O. Bubulac, R. E. De Wames, J.Electron. Mater. **22**(8), 1039 (1993).

© 2004 WILEY-VCH Verlag GmbH & Co. KGaA, Weinheim